PET Findings of Intramedullary Tumors of the Spinal Cord Using [^{18}F] FDG and [^{11}C] Methionine

N. Tomura, Y. Ito, H. Matsuoka, T. Saginoya, S.-i. Numazawa, Y. Mizuno, and K. Watanabe

ABSTRACT

BACKGROUND AND PURPOSE: Only a few reports on intramedullary tumors of the spinal cord using PET have been published. We report findings of PET by using [^{18}F] fluorodeoxyglucose and [^{11}C] methionine and discuss the usefulness of the findings in patients with intramedullary tumors of the spinal cord.

MATERIALS AND METHODS: PET/CT was performed in 9 patients with intramedullary tumors of the spinal cord: Six had ependymomas, 1 had an anaplastic astrocytoma, 1 had a hemangioblastoma, and 1 had a cavernous angioma. The maximum standardized uptake value of the tumor was measured and compared with pathologic findings.

RESULTS: The SUVmax of FDG and MET in a case of anaplastic astrocytoma was high. The SUVmax of FDG and MET was relatively high in 4 of 6 cases of ependymoma (excluding myxopapillary ependymomas). A case of hemangioblastoma showed decreased uptake of both FDG and MET (SUVmax = 2.0 and 1.4, respectively). Three cases with hemorrhage (1 case of ependymoma, 1 case of cellular ependymoma, and 1 case of cavernous angioma) showed a relatively increased uptake of FDG.

CONCLUSIONS: Both FDG and MET accumulated to a large degree in an anaplastic astrocytoma and accumulated in ependymomas (excluding a myxopapillary ependymoma). FDG can accumulate in tumors with hemorrhage. More investigation of a larger number of patients is required to evaluate the diagnostic value of PET with FDG and MET for imaging intramedullary tumors of the spinal cord.

ABBREVIATIONS: [^{11}C] = carbon 11; [^{18}F] = fluorine 18; FDG = fluorodeoxyglucose; MET = ^{11}C methionine; SUVmax = maximum standardized uptake value

PET has been used to evaluate the grade of malignant brain tumors[1-3] and to differentiate recurrent tumors from radiation necrosis after radiation therapy.[4-7] In other regions, PET has been used to detect neoplastic lesions such as metastatic ones and to differentiate neoplastic from non-neoplastic lesions.[8-12] PET has also been used to evaluate the therapeutic response of brain tumors[13,14] and other tumors.[15-17] [^{18}F]-fluorodeoxyglucose and [^{11}C] methionine have been generally used as tracers for neoplasms.[18] Numerous imaging tracer studies have been reported for diseases in the brain; however, only a few reports on intramedullary tumors of the spinal cord have been published.[19-26] A majority of these previously published reports were case reports that included ependymomas, glioblastomas, and so forth. The present study included 9 patients with intramedullary tumors, and the PET findings by using FDG and MET are reviewed.

MATERIALS AND METHODS

Patients

Subjects included 9 patients with intramedullary tumors of the spinal cord. They included 4 males and 5 females, and their ages ranged from 12 to 75 years, with a mean age of 36.8 years. This study was approved by the institutional review board of our hospital, and every patient gave written informed consent before their study. The public insurance system in our country permits only FDG-PET, so MET-PET was performed together with FDG-PET in every patient. The tumor was located in the cervical cord in 3 patients, in the thoracic cord in 3 patients, and in the lumbar cord in 3 patients. In every patient, the pathology of the tumor was proved by surgery after PET/CT. Total removal of the tumor was performed in 7 cases, and partial removal was performed in 1 case. Biopsy was performed in 1 case of an anaplastic astrocytoma. Pathology included in anaplastic astrocytoma (n = 1), ependymomas (n = 6; 2 ependymomas, 1 tanycytic ependymoma, 2 myxopapillary ependymomas, and 1 cellular

Received June 14, 2012; accepted after revision August 14.

From the Departments of Radiology (N.T., T.S., Y.M.) and Neurosurgery (Y.I., H.M., S.-i.N., K.W.), Southern Tohoku Research Institute for Neuroscience, Southern Tohoku General Hospital, Fukushima, Japan.

Please address correspondence to Noriaki Tomura, MD, Department of Radiology, Southern Tohoku Research Institute for Neuroscience, Southern Tohoku General Hospital, 7–115, Yatsuyamada, Koriyama, Fukushima, 963-8563, Japan; e-mail: tomura@bloom.ocn.ne.jp

http://dx.doi.org/10.3174/ajnr.A3374

SUVmax of each tumor

Patient	Age (yr)	Sex	Pathology	Location	Cystic Component	SUVmax (FDG)	SUVmax (MET)
1	23	F	Anaplastic astrocytoma	Th	–	7.4	3.2
2	47	M	Hemangioblastoma	L	+	2.5	2.4
3	18	F	Ependymoma	C	+	10	2.9
4	56	M	Ependymoma	C	+	11.2	2.2
5	30	M	Ependymoma (myxopapillary)	L	+	2.4	2.2
6	41	M	Ependymoma (tanycytic)	Th	–	5.4	2.4
7	12	F	Cavernous angioma	Th	–	5.2	2.0
8	75	F	Ependymoma (cellular)	C	+	7.1	3.5
9	29	F	Ependymoma (myxopapillary)	L	+	3.5	3.2

Note:—Th indicates thoracic cord; L, lumbar cord; C, cervical cord; –, absence of cystic component on MRI; +, existence of cystic component on MRI.

ependymoma), a hemangioblastoma ($n = 1$), and a cavernous angioma ($n = 1$).

Imaging

Plasma glucose was checked before the PET/CT examination and was <103 mg/dL in all patients. PET/CT by using both FDG and MET was performed in all patients. PET/CT examinations were performed by using 2 different PET/CT units. Full width at half maximum axial spatial resolution was 6 mm with 1 unit and 7 mm with another unit. CT was performed by using a continuous spiral technique with a 4- or 16-section spiral CT that had a gantry rotation speed of 0.8 seconds. CT was performed at 10, 250, or 300 mAs; 120 KeV; with a section width of 3.75 or 5.0 mm; and a table feed of 18.75, 15.0, 11.25, or 7.5 mm per rotation. No intravenous contrast material was used. After CT, PET using MET was performed 20 minutes after injection of MET (325.8–643.9 MBq). For PET using FDG, FDG was injected 60 minutes after MET-PET. FDG-PET was performed 60 minutes after injection of FDG (145.2–237.9 MBq). The acquisition time was 5 or 10 minutes per table position. PET images were reconstructed by using CT data for attenuation correction and image fusion.

Coregistered images were displayed on a workstation. The maximum standardized uptake value of the tumor was measured by placing a circular region of interest over the area including the maximum uptake, and the SUVmax was compared with pathologic findings. One of the authors (N.T.) placed ROIs to measure SUVmax in every patient. The size of the region of interest ranged from 30.5 to 366.2 mm^2.

All patients underwent MR imaging, including T2-, T1-, and contrast-enhanced T1-weighted imaging with or without fat saturation within 5 days of the PET/CT. Scan parameters were as follows: fast spin-echo T1WI with or without fat saturation, TR = 600–660 ms; TE = 9.856–16.596 ms; section thickness = 3.0–5.0 mm; section gap = 0.5–1.0 mm; NEX = 1 or 1.5; FOV = 15–38 cm; and matrix = 256–320 × 128–224; and fast spin-echo T2WI, TR = 3000–4500 ms; TE = 110.64–121.968 ms; section thickness = 3.0–5.0 mm; section gap = 0.5–1.0 mm; NEX = 1 or 1.5; FOV = 15–38 cm; and matrix = 256–320 × 128–224. Fusion images of PET with MR imaging were made at a workstation. The location of contrast enhancement of the tumor was compared between tumor uptake of FDG and MET.

RESULTS

PET findings are shown in the Table. The SUVmax of FDG and MET in a case of anaplastic astrocytoma was 7.4 and 3.2, respectively (Fig 1). In cases of ependymoma, the SUVmax of MET was variable in all cases, and the SUVmax of FDG was relatively high in 4 cases (Fig 2). Two cases of myxopapillary ependymoma exhibited a decreased uptake of FDG (2.4 and 3.5). A case of hemangioblastoma showed decreased uptake of both FDG and MET (2.5 and 2.4, respectively). In a case of cavernous angioma, though the SUVmax of MET was low (2.0), that of FDG was relatively high (5.2) (Fig 3). Three of 4 patients with hemorrhage on pathology (patients 2, 4, 7, and 8 in the Table) showed increased uptake of FDG. Contrast-enhanced T1-weighted images showed variable degrees of contrast enhancement in a part of the tumor, which was almost compatible with the activated area seen with FDG and MET.

DISCUSSION

In contrast to numerous reports that have used PET to image intracranial tumors, reports using PET to image primary intramedullary tumors of the spinal cord have been limited. A reason for this lack of reports may be partly due to the poor resolution of PET. However, the resolution of PET has recently improved greatly, and PET/CT can now allow confirmation of spinal cord tumor location within the vertebral column. In the present study, PET/CT images superimposed on MR images were also reviewed. A recent review of the literature revealed 8 reports using PET for primary intramedullary tumors of the spinal cord from 1983 to 2009.[19-26] Six of these are case reports that included a ganglioneuroma, ependymomas, a glioblastoma, a primitive neuroectodermal tumor, an oligoastrocytoma, and a hemangioma. Two of these 6 tumors were ependymomas examined with MET-PET, and the other 4 tumors were examined by FDG-PET. All 6 of those tumors exhibited a slight-to-moderate uptake of FDG or MET. Two malignant tumors among those reported cases, a glioblastoma and a primitive neuroectodermal tumor, revealed an increased uptake of FDG.

Wilmshurst et al[24] reported the use of FDG-PET or MET-PET before or after therapy in 14 patients with a primary intramedullary tumor. In their study, FDG-PET was performed in 7 tumors, and MET-PET was performed in 1 tumor before therapy. Other PET examinations were performed after surgery and/or radiation therapy. An ependymoma exhibited low uptake (SUV = 2.2), and another ependymoma showed increased uptake (SUV was not indicated) of FDG. Only 1 MET-PET image in their study was performed in a patient with a ganglioglioma. That ganglioglioma exhibited low uptake (SUV = 1.7). Although they reported PET

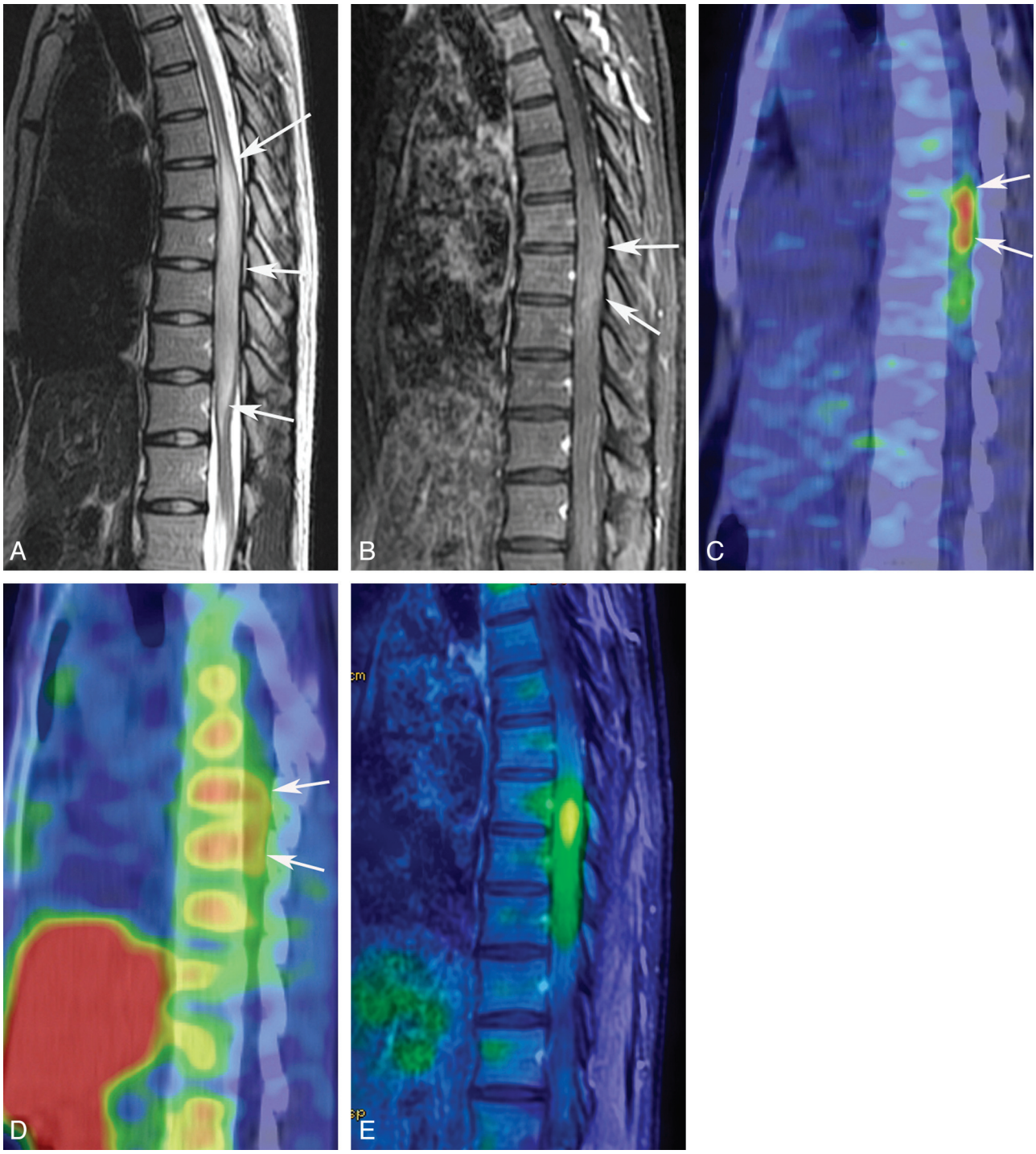

FIG 1. A 23-year-old woman with an anaplastic astrocytoma. T2-weighted MR image (*A*) reveals a tumor of the spinal cord from the eighth thoracic vertebra to the first lumbar vertebra (*white arrows*). A contrast-enhanced T1-weighted MR image with fat saturation (*B*) shows mild contrast enhancement of the tumor (*white arrows*). FDG-PET (*C*) and MET-PET (*D*) reveal increased activity of both FDG (SUVmax = 7.4) and MET (SUVmax = 3.2) of the tumor (*white arrows*). A fusion image of FDG-PET and contrast-enhanced T1-weighted MR imaging with fat saturation (*E*) clearly shows increased uptake of FDG in the tumor.

findings after therapy, PET findings in patients after radiation therapy are greatly influenced by postradiation changes.

The present imaging study was performed before therapy in all patients, and both FDG-PET and MET-PET were performed at the same time. A patient with an anaplastic astrocytoma with a high-grade glioma of the spinal cord underwent PET before therapy and exhibited the highest uptake of both FDG and MET in the present series. As in intracranial tumors, increased uptake of both FDG and MET might be of diagnostic value.

For imaging intramedullary tumors of the spinal cord, FDG seemed superior to MET because the uptake value of FDG was higher than that of MET for every tumor in the present study. Unlike intracranial brain tissue, no increased uptake of FDG is evident in the normal spinal cord. Accumulation of MET in the

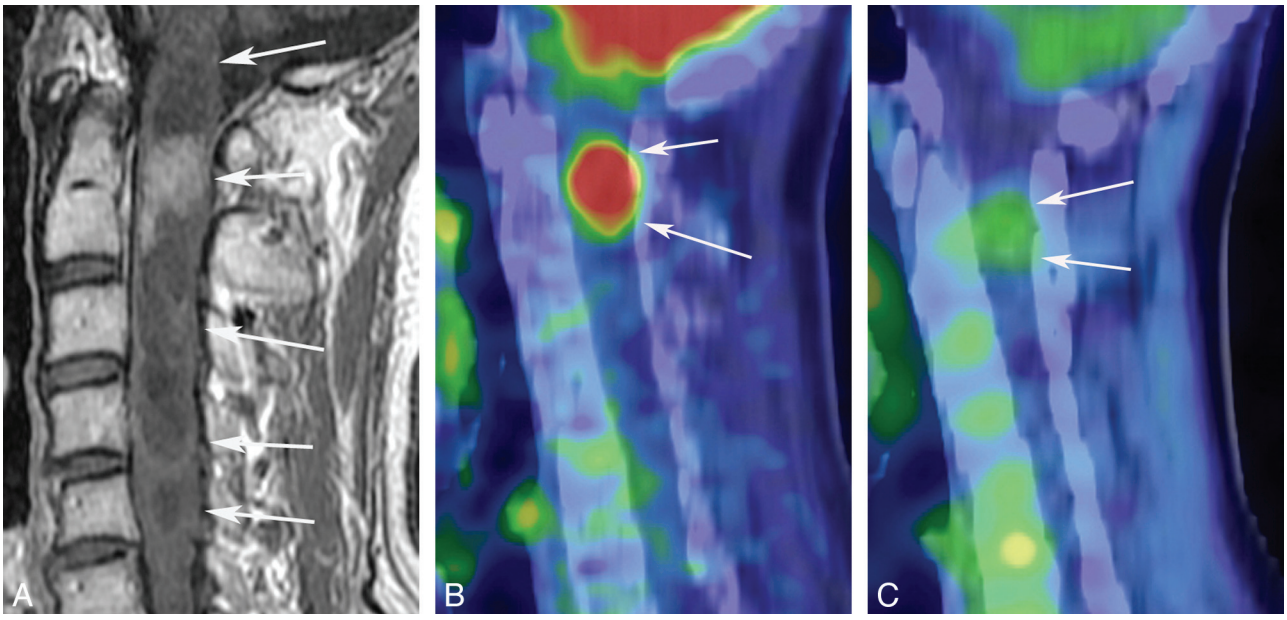

FIG 2. A 56-year-old man with an ependymoma. A contrast-enhanced T1-weighted image (*A*) shows a tumor from the first to fifth cervical vertebra with a cystic and solid component (*white arrows*). Contrast enhancement of the solid component at the second cervical vertebra is seen (*white arrows*). FDG-PET (*B*) and MET-PET (*C*) show accumulation of both FDG (SUVmax = 11.2) and MET (SUVmax = 2.2) (*white arrows*).

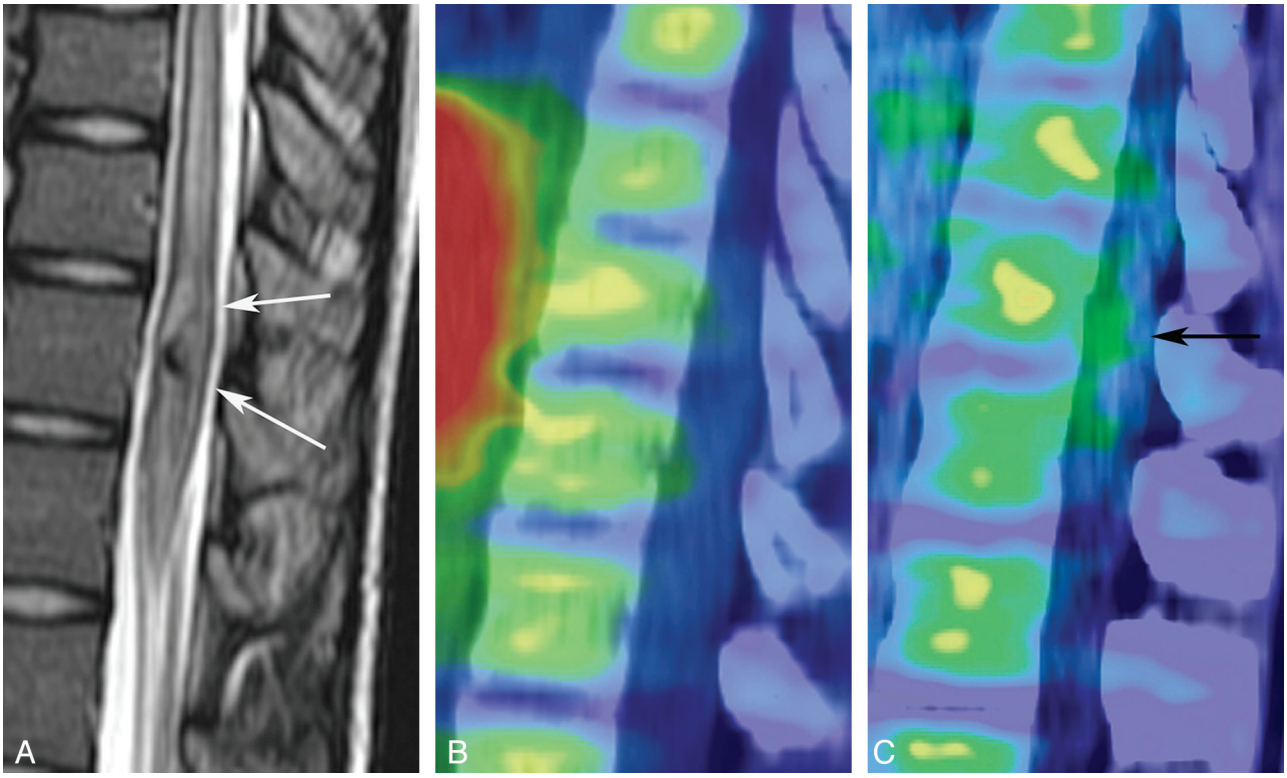

FIG 3. A 12-year-old girl with a cavernous angioma. A T2-weighted MR image (*A*) shows a mainly hypointense tumor (*white arrows*) at the twelfth thoracic vertebra. Hypointensity may be due to hemosiderin deposition. A hyperintense area surrounding the hypointense lesion seems to be edema, but its histologic evidence was not acquired. Although accumulation of MET is not evident (*B*), FDG-PET (*C*) shows slight activity of the tumor (SUVmax = 5.2) (*black arrow*).

vertebral body may somewhat disturb visualization of mild tumor uptake of MET. The partial volume effect from the activity of MET in the vertebral body seems to influence the SUV of MET in the tumors. Fusion images of PET and MR imaging, used in the present study, could be useful to discriminate mild tumor uptake of MET. Recently developed PET-MR imaging[27] would be feasible to image those tumors with mild uptake.

MET uptake was decreased in the cavernous angioma, which was not exactly classified into the neoplasms. MET may be more useful than FDG in differentiation of neoplastic and non-neoplas-

tic diseases. Comparison of the clinical significance of FDG with that of MET, for example, in the evaluation of treatment response, staging, and differentiation of malignant tumors from benign lesions, should be investigated further. All tumors exhibited enhancement of the tumor on contrast-enhanced MR imaging. Accumulation of both FDG and MET corresponded well with the location of contrast enhancement on MR imaging. The mechanism of accumulation of both FDG and MET in the tumor may be partly due to disruption of the blood–spinal cord barrier of the tumor and to the increased blood volume of the tumor. As with other mechanisms of uptake of MET into the tumor, increased carrier-mediated transport and elevated protein synthesis have been reported.[28,29] Kracht et al[30] reported a correlation between MET uptake in glioma and microvessel attenuation. The increased expression of amino acid transporters may be presumably on endothelial cells of newly formed tumor vessels. FDG uptake is also a complex mechanism, reflecting both glucose transport and consumption and providing indications concerning the biologic status of the tumor. Glucose consumption is related to grading of the tumor, cell attenuation, and biologic aggressiveness.[29]

SUVmax was used as a marker of activity of FDG and MET in each tumor.[18,31] In the brain, comparison of uptake of the lesion with uptake in the unaffected hemisphere has been used[32-34]; however, this comparison cannot be used in the spinal cord. SUV is dependent on the timing between injection of the tracer and imaging. There may be a small difference in SUV between the present study and the study by Wilmshurst et al[24] because the timing of FDG and MET imaging from the injection in the present study slightly differed from that in their study. In the present study, SUVmax was used; however, use of the mean or minimum SUV is controversial. In many tumors with a cystic component, the minimum or mean SUV may not be practical.

In the present study, 6 of 9 tumors were ependymomas. Two of these 6 ependymomas were myxopapillary ependymomas, both of which showed low uptake of FDG. Ependymomas, including tanycytic and cellular ependymomas and exclusive of myxopapillary ependymomas, showed increased uptake of FDG. Absence of increased uptake of FDG in myxopapillary ependymomas may be useful for differentiation between myxopapillary ependymomas and other histologic types of ependymomas. Differences in uptake between myxopapillary and other histologic types of ependymomas could be diagnostically useful because prognosis of myxopapillary ependymomas somewhat differs from that of other histologic types of ependymomas.[35] Another common intramedullary tumor of the spinal cord is an astrocytoma. No low-grade astrocytomas were examined in our series. In the study by Wilmshurst et al,[24] 4 low-grade astrocytomas showed a slight or moderate uptake of FDG before treatment. No ependymomas were studied before treatment in their study. SUV of both FDG and MET is probably not crucial for differentiation of astrocytomas and ependymomas.

Previous reports of imaging of intracranial hemangioblastomas have shown a low uptake of FDG or MET, as was seen in the present report.[36] Only 1 report[26] of imaging a cavernous angioma of the spinal cord by using PET has been found. It showed low-grade uptake of FDG to the lesion. The present report did not show remarkable uptake of MET but did show moderate uptake of FDG in the cavernous angioma. In the present study, 3 tumors with hemorrhage, including a cavernous angioma, showed a relatively increased uptake of FDG. In previously reported cases with intracerebral hematoma, Powers[37] and Allyson et al[38] reported increased uptake of FDG in the area surrounding the intracerebral hematoma. All tumors with hemorrhage reported in the present study showed microscopic hemorrhages without evidence of subacute hemorrhage. The mechanism of accumulation of FDG is unknown; however, it may be related to mononuclear perivascular infiltrates, gliosis, and activated macrophages.[39] Increased activity of mononuclear cells and glial cells may augment consumption of FDG. These microscopic findings were not evident in our series. Susceptibility-weighted images may be useful for evaluating the existence of hemorrhage within the lesion when interpreting the FDG-PET results. The relationships of uptake of MET or FDG to hemorrhage must be further investigated.

Wilmshurst et al[24] also remarked that both FDG-PET and MET-PET did not provide more information beyond what is provided by MR imaging in the diagnosis of spinal cord tumors. However, a remarkably increased uptake of both FDG and MET, seen in an anaplastic astrocytoma in the present series, could be used to diagnose high-grade or malignant tumors. The clinical usefulness of FDG-PET and MET-PET compared with MR imaging for the evaluation of treatment response, differentiation between recurrent tumor and radiation necrosis, and differential diagnosis of neoplastic from non-neoplastic lesions should be further investigated in more patients, including those with low-grade astrocytomas; and it is also necessary to study this usefulness in other lesions such as inflammatory and demyelinating processes. As in the brain, FDG can also accumulate in inflammatory lesions of the spinal cord. FDG has been observed accumulated in leukocytes, lymphocytes, and macrophages in vitro.[11] An increased FDG distribution level was observed in granulomas, whereas MET distribution level was low.[11] In patients with neoplasms in the brain, PET by using FDG or MET is more feasible than MR imaging for follow-up therapeutic results. In patients with neoplasms in the spinal cord, PET could be feasible for follow-up after therapy such as surgery, radiation, or chemotherapy.

Postoperative changes and changes after therapy make it difficult to evaluate recurrent diseases, even if contrast-enhanced MR imaging is performed. In patients diagnosed with benign astrocytomas or ependymomas by MR imaging, PET could also be helpful for follow-up because a tendency for increased uptake may indicate malignant transformation of the tumor. MR perfusion and CTP can show blood flow and blood volume of the tumors in the brain; however, they may not clearly give us functional images due to relatively small lesions of the spinal cord. Compared with MR imaging, PET has a limitation of radiation exposure, especially for pediatric and young patients. In our country, FDG-PET does not necessarily need the cyclotron because FDG is commercially available, but the cyclotron is necessary to produce MET in the hospital. PET examinations need more time for scanning than MR imaging.

There are limitations to the present study. The biggest limitation is the small number of subjects, though the present study was performed in a larger number of subjects than has been previously reported. Low-grade astrocytomas were not included, and only 1

high-grade astrocytoma was examined. Other kinds of intramedullary tumors such as subependymomas, gangliogliomas, lymphomas, and oligodendrogliomas should be investigated.

CONCLUSIONS

Both FDG and MET accumulated significantly in anaplastic astrocytomas. FDG and MET also accumulated in ependymomas (excluding the myxopapillary subtype). FDG could accumulate in tumors with hemorrhage. The present study could not confirm that either FDG-PET or MET-PET provides more information in the diagnosis of intramedullary tumors of the spinal cord compared with MR imaging. Further investigation into a larger number of patients is required to determine the value of FDG-PET and MET-PET in diagnosis, clinical evaluation of treatment response, differentiation between recurrent tumor and radiation necrosis, and differential diagnosis of neoplastic from non-neoplastic lesions.

REFERENCES

1. Borgwardt L, Højgaard L, Carstensen H, et al. **Increased fluorine-18–2-fluoro-2-deoxy-D-glucose (FDG) uptake in childhood CNS tumors is correlated with malignancy grade: a study with FDG positron emission tomography/magnetic resonance imaging coregistration and image fusion.** *J Clin Oncol* 2005;23:3030–37
2. Choi SJ, Kim JS, Kim JH, et al. **[18F]3′-deoxy-3′-fluorothymidine PET for the diagnosis and grading of brain tumors.** *Eur J Nucl Med Mol Imaging* 2005;32:653–59
3. Tsuchida T, Takeuchi H, Okazawa H, et al. **Grading of brain glioma with 1-^{11}C-acetate PET: comparison with ^{18}F-FDG PET.** *Nucl Med Biol* 2008;35:171–76
4. Hustinx R, Pourdehnad M, Kaschten B, et al. **PET imaging for differentiating recurrent brain tumor from radiation necrosis.** *Radiol Clin North Am* 2005;43:35–47
5. Terakawa Y, Tsuyuguchi N, Iwai Y, et al. **Diagnostic accuracy of ^{11}C-methionine PET for differentiation of recurrent brain tumors from radiation necrosis after radiotherapy.** *J Nucl Med* 2008;49:694–99
6. Kim YH, Oh SW, Lim YJ, et al. **Differentiating radiation necrosis from tumor recurrence in high-grade gliomas: assessing the efficacy of ^{18}F-FDG PET, ^{11}C-methionine PET and perfusion MRI.** *Clin Neurol Neurosurg* 2010;112:758–65
7. Tan H, Chen L, Guan Y, et al. **Comparison of MRI, F-18 FDG, and C-11 choline PET/CT for their potentials in differentiating brain tumor recurrence from brain tumor necrosis following radiotherapy.** *Clin Nucl Med* 2011;36:978–81
8. Wong TZ, van der Westhuizen GJ, Coleman RE. **Positron emission tomography imaging of brain tumors.** *Neuroimaging Clin N Am* 2002;12:615–26
9. Salaun PY, Gastinne T, Bodet-Milin C, et al. **Analysis of ^{18}F-FDG PET diffuse bone marrow uptake and splenic uptake in staging of Hodgkin's lymphoma: a reflection of disease infiltration or just inflammation?** *Eur J Nucl Med Mol Imaging* 2009;36:1813–21
10. Smeets P, Ham H, Ceelen W, et al. **Differentiation between perianastomotic inflammatory changes and local recurrence following neoadjuvant radiochemotherapy surgery for colorectal cancer using visual and semiquantitative analysis of PET-CT data.** *Q J Nucl Med Mol Imaging* 2010;54:327–32
11. Zhao S, Kuge Y, Kohanawa M, et al. **Usefulness of ^{11}C-methionine for differentiating tumors from granulomas in experimental rat models: a comparison with ^{18}F-FDG and ^{18}F-FLT.** *J Nucl Med* 2008;49:135–41
12. Phi JH, Paeng JC, Lee HS, et al. **Evaluation of focal cortical dysplasia and mixed neuronal and glial tumors in pediatric epilepsy patients using ^{18}F-FDG and ^{11}C-methionine PET.** *J Nucl Med* 2010;51:728–34
13. Kawai N, Miyake K, Yamamoto Y, et al. **Use of ^{11}C-methionine positron emission tomography in basal germinoma: assessment of treatment response and residual tumor.** *Childs Nerv Syst* 2009;25:845–53
14. Piroth MD, Pinkawa M, Holy R, et al. **Prognostic value of early [^{18}F]fluoroethyltyrosine positron emission tomography after radiochemotherapy in glioblastoma multiforme.** *Int J Radiat Oncol Biol Phys* 2011;80:176–84
15. Palma P, Conde-Muino R, Rodriguez-Fernandez A, et al. **The value of metabolic imaging to predict tumour response after chemoradiation in locally advanced rectal cancer.** *Radiat Oncol* 2010;5:119
16. Aukema TS, Kappers I, Valdes Olmos RA, et al. **Is ^{18}F-FDG PET/CT useful for the early prediction of histopathologic response to neoadjuvant erlotinib in patients with non-small cell lung cancer?** *J Nucl Med* 2010;51:1344–48
17. Singnurkar A, Solomon SB, Gönen M, et al. **^{18}F-FDG PET/CT for the prediction and detection of local recurrence after radiofrequency ablation of malignant lung lesions.** *J Nucl Med* 2010;51:1833–40
18. Kapoor V, McCook BM, Torok FS. **An introducing to PET-CT imaging.** *Radiographics* 2004;24:523–43
19. Di Chiro G, Edward O, Bairamian E, et al. **Metabolic imaging of the brain stem and spinal cord: studies with positron emission tomography using ^{18}F-2-deoxyglucose in normal and pathological cases.** *J Comput Assist Tomogr* 1983;7:937–45
20. Higano S, Shishido F, Nagashima M, et al. **PET evaluation of spinal cord tumor using ^{11}C-methionine.** *J Comput Assist Tomogr* 1990;14:297–99
21. Alavi A, Kramer E, Wegener W, et al. **Magnetic resonance and fluorine-18 deoxyglucose imaging in the investigation of a spinal cord tumor.** *J Nucl Med* 1990;31:360–64
22. Sasajima T, Mineura K, Itoh Y, et al. **Spinal cord ependymoma: a positron emission tomographic study with (^{11}C-methyl)-L-methionine.** *Neuroradiology* 1996;38:53–55
23. Meltzer CC, Townsend DW, Kottapally S, et al. **FDG imaging of spinal cord primitive neuroectodermal tumor.** *J Nucl Med* 1998;39:1207–09
24. Wilmshurst JM, Barrington SF, Pritchard D, et al. **Positron emission tomography in imaging spinal cord tumors.** *J Child Neurol* 2000;15:465–72
25. Shimizu T, Saito N, Aihara M, et al. **Primary spinal oligoastrocytoma: a case report.** *Surg Neurol* 2004;61:77–81
26. D'Souza MM, Sharma R, Tripathi M, et al. **Unusual diagnosis of von Hippel Lindau syndrome on PET/CT. Case report and brief review of literature.** *Iran J Nucl Med* 2009;17:50–54
27. Herzog H, Van Den Hoff J. **Combined PET/MR systems: an overview and comparison of currently available options.** *Q J Nucl Med Mol Imaging* 2012;56:247–67
28. Jacobs AH, Thomas A, Kracht LW, et al. **^{18}F-fluoro-L-thymidine and ^{11}C-methylmethionine as markers of increased transport and proliferation in brain tumors.** *J Nucl Med* 2005;46:1948–58
29. Viel T, Talasila KM, Monfared P, et al. **Analysis of the growth dynamics of angiogenesis-dependent and –independent experimental glioblastomas by multimodal small-animal PET and MRI.** *J Nucl Med* 2012;53:1135–45
30. Kracht LW, Friese M, Herholz K, et al. **Methyl-[^{11}C]-methyonine uptake as measured by positron emission tomography correlates to microvessel density in patients with glioma.** *Eur J Nucl Med Mol Imaging* 2003;30:868–73
31. Thie JA. **Understanding the standardized uptake value, its methods, and implications for usage.** *J Nucl Med* 2004;45:1431–34
32. Gumprecht H, Grosu AL, Souvatsoglou M, et al. **^{11}C-methionine positron emission tomography for preoperative evaluation of suggestive low-grade gliomas.** *Zentralbl Neurochir* 2007;68:19–23
33. Kato T, Shinoda J, Oka N, et al. **Analysis of 11C-methionine uptake in low-grade gliomas and correlation with proliferative activity.** *AJNR Am J Neuroradiol* 2008;29:1867–71
34. Kawase Y, Yamamoto Y, Kameyama R, et al. **Comparison of ^{11}C-methionine PET and ^{18}F-FDG PET in patients with primary central nervous system lymphoma.** *Mol Imaging Biol* 2011;13:1284–89
35. Fassett DR, Pingree J, Kestle JR. **The high incidence of tumor dissemination in myxopapillary ependymoma in pediatric patients: report of five cases and review of the literature.** *J Neurosurg* 2005;102:59–64
36. Morooka M, Ito K, Kubota K, et al. **^{11}C-choline and F-18 FDG PET/CT images of hemangioblastoma.** *Clin Nucl Med* 2011;36:143–44
37. Powers WJ. **Intracerebral hemorrhage and head trauma and common effects and common mechanisms of injury.** *Stroke* 2010;41(10 suppl):S107–10
38. Allyson R, Zazulia AR, Videen TO, et al. **Transient focal increase in perihematomal glucose metabolism after acute human intracerebral hemorrhage.** *Stroke* 2009;40:1638–43
39. Bleeker-Rovers CP, Vos FJ, Corstens HM, et al. **Imaging of infectious disease using [^{18}F]fluorodeoxyglucose PET.** *Q J Nucl Med Mol Imaging* 2008;52:17–29